Accelerated Dynamic MRI Reconstruction with Total Variation and Nuclear Norm Regularization*

Jiawen Yao[1], Zheng Xu[1], Xiaolei Huang[2], and Junzhou Huang[1,**]

[1] Department of Computer Science and Engineering, University of Texas at Arlington, Arlington TX 76019, USA
[2] Computer Science and Engineering Department, Lehigh University, Bethlehem, PA 18015, USA
jzhuang@uta.edu

Abstract. In this paper, we propose a novel compressive sensing model for dynamic MR reconstruction. With total variation (TV) and nuclear norm (NN) regularization, our method can utilize both spatial and temporal redundancy in dynamic MR images. Due to the non-smoothness and non-separability of TV and NN terms, it is difficult to optimize the primal problem. To address this issue, we propose a fast algorithm by solving a primal-dual form of the original problem. The ergodic convergence rate of the proposed method is $\mathcal{O}(1/N)$ for N iterations. In comparison with six state-of-the-art methods, extensive experiments on single-coil and multi-coil dynamic MR data demonstrate the superior performance of the proposed method in terms of both reconstruction accuracy and time complexity.

1 Introduction

Dynamic magnetic resonance imaging (dMRI) is an important medical imaging technique that has been widely used for multiple clinical applications. To reduce scanning time, partial k-space data are typically required for reconstruction instead of full sampling. However, when k-space is under sampled, the Nyquist criterion is violated and the inverse Fourier transform will exhibit aliasing artifacts. Fortunately, dynamic MR sequences often provide both redundant spatial and temporal information, which makes the use of Compressive Sensing (CS) theory repeatedly successful [6,14,13].

There are two kinds of prior knowledge about dynamic MR images which can be used by CS methods. First, a dynamic MR sequence has the piece-wise smooth property in the spatial domain. In traditional CS-MRI reconstructions, the piecewise smooth property of MR images plays a very important role. With the sparsity-induced regularization such as Wavelets [13] or Total Variation [9,8], it is possible to reconstruct high quality MR images using far fewer measurements.

* This work was partially supported by U.S. NSF IIS-1423056, CMMI-1434401, CNS-1405985.

** Corresponding author.

N. Navab et al. (Eds.): MICCAI 2015, Part II, LNCS 9350, pp. 635–642, 2015.
DOI: 10.1007/978-3-319-24571-3_76

Second, dynamic MR images actually are temporally correlated due to very slow changes of the same organ(s) through the whole image sequence. Such high correlation in the temporal domain becomes another piece of important prior knowledge for guiding dynamic MRI reconstruction.

In recent years, researchers have proposed two types of dMRI reconstructions based on temporal information of dynamic MR images. The first type of methods applies a sparsity constraint in the temporal domain, e.g. Dictionary Learning with Temporal Gradients (DLTG) [2] and Dynamic Total Variation (DTV) [5]. Instead of using sparsity in the temporal domain, another type of methods exploits the low-rank property of matrices. Based on rank minimization, low-rank plus sparse decomposition methods are proposed for dMRI reconstruction [16,18]. Because these methods collect the data from all frames in the reconstruction, they can exploit the redundancies of the whole dataset and reconstruct more accurate results. However, drawbacks are their sensitivity to noise. They may fail in recovering clean images when the acquired data are contaminated with noise because the sparse prior cannot exploit the local spatial consistency or piece-wise smoothness of dynamic MR images.

In this paper, by exploiting redundancies in both the temporal and spatial domains, we propose a Total Variation and Nuclear Norm Regularization (TVNNR) model for dMRI reconstruction. In our TVNNR, nuclear norm (NN) exploits the low-rank property of dynamic MR images while total variation encourages each MR frame's intensities to be locally consistent which can enforce the piece-wise smoothness constraint and make reconstruction more robust to noise. The intuition of combining TV and NN terms is simple, but the joint TV/NN minimization problem is actually difficult to solve because of the non-separability and non-smoothness of the two terms. A fast algorithm (FTVNNR) is then proposed to efficiently solve this problem. It can obtain a $\mathcal{O}(1/N)$ convergence rate for N iterations. Extensive experiments on dynamic MR data demonstrate its superior performance over all previous methods in terms of both reconstruction accuracy and computational complexity.

2 Model

Here we assume $x_1, ..., x_T$ as one dynamic MR sequence to be reconstructed. At time t, $x_t \in \mathbb{C}^{m \times n}$ is one dynamic MR frame, the physical model for the undersampled k-space measurement of x_t can be formulated as

$$b_t = R_t(Fx_t + n), \tag{1}$$

where b_t is the measurement vector which may contain noise (n represents noise in k-space); R_t denotes the undersampling mask to acquire only a subset of k-space and F performs a 2D Discrete Fourier Transform (DFT).

With prior knowledge in the temporal and spatial domains, it is possible to reconstruct x_t with fewer k-space measurements b_t. Based on a batch scheme, the proposed TVNNR model for dMRI reconstruction is defined as follows

$$\min_X \frac{1}{2}||RFX - B||_F^2 + \lambda_1||X||_{TV} + \lambda_2||X||_*, \tag{2}$$

where $X \in \mathbb{R}^{mn\times t}$ denotes the whole dynamic MR images. $||X||_*$ is the nuclear norm—the sum of singular values of the matrix X. $||X||_{TV}$ denotes the anisotropic total variation of the matrix X. It is defined as $\sum_{t=1}^{T}\sum_{ij}(|\nabla_1 x_{i,j,t}| + |\nabla_2 x_{i,j,t}|)$ where ∇_1 and ∇_2 denote the forward finite difference operators on the first and second coordinates, respectively. If we define $\nabla = [\nabla_1, \nabla_2]$, $||X||_{TV}$ can be simplified as $\|\nabla X\|_1$. $B = [b_1, b_2, ..., b_T]^T$ represents the collection of all the measurements.

Although the problem (2) is the single coil case, it has the potential to process multi-coil parallel MRI data. When the coil sensitivities are available, it can be combined with SENSE in the k-t SPARSE-SENSE framework [17] by multiplying coil sensitivities E after the undersampled Fourier transform, which means the least square term in (2) will be $||RFEX - B||_F^2$.

3 Algorithm

Due to the non-smoothness and non-separability of both the TV and NN functions, it is very difficult to efficiently solve the primal problem (2). Instead of directly solving the primal problem, it is suggested in [3,4] that TV regularization can be solved by its dual form. By using the Legendre-Fenchel transformation of total variation (see Ref. [1], Example. 3. 26, p. 93), we can have the primal-dual form of the primal problem (2) as

$$\min_X \max_Y \frac{1}{2}\|RFX - B\|_F^2 + \lambda_2\|X\|_* + \lambda_1\langle \nabla X, Y\rangle - I_{B_\infty}(Y), \tag{3}$$

where Y is the dual variable and $I_{B_\infty}(Y)$ is the indicator function of the ℓ_∞ unit norm ball

$$I_{B_\infty}(Y) = \begin{cases} 0 & \|Y\|_\infty \le 1, \\ +\infty & \text{otherwise.} \end{cases} \tag{4}$$

The min-max problem (3) can be solved by a splitting scheme [7] as

$$X^{n+1} = \arg\min_X \frac{1}{2}\|X - X^n\|_F^2 + \frac{t_1}{2}\|RFX - B\|_F^2 + t_1\lambda_1\langle \nabla X, Y^n\rangle + t_1\lambda_2\|X\|_* \tag{5}$$

$$Y^{n+1} = \arg\min_Y \frac{1}{2}\|Y - Y^n\|_F^2 + I_{B_\infty}(Y) - t_2\lambda_1\langle \nabla(2X^{n+1} - X^n), Y\rangle, \tag{6}$$

where X^n, Y^n are the primal and dual variables in the n-th iteration, respectively. t_1, t_2 are the corresponding iteration step sizes.

First, for the X **subproblem** (5), it can be reduced to a de-noising problem by [4] as

$$X^{n+1} = \arg\min_X \frac{1}{2}\|X - \bar{X}^n\|_F^2 + \lambda\|X\|_*, \tag{7}$$

where

$$\bar{X}^n = X^n - \frac{t_1}{1 + t_1 L}\mathcal{A}^T(\mathcal{A}X^n - B) - \frac{t_1\lambda_1}{1 + t_1 L}\nabla^T Y^n, \quad \lambda = \frac{t_1\lambda_2}{1 + t_1 L}.$$

Here $\mathcal{A} = RF$ and $L = \lambda_{max}(\mathcal{A}^T\mathcal{A})$. ∇^T is the adjoint operator of ∇. Suppose that $\bar{X}^n = Udiag(\sigma(\bar{X}^n))V^H$ is any singular value decomposition of $\bar{X}^n$. Then the solution of (7) can be obtained by the matrix shrinkage operator [15] as $X^{n+1} = S_\lambda(\bar{X}^n) = Udiag(\overline{\sigma}_\lambda(\bar{X}^n))V^H$ where $\overline{\sigma}_\lambda(\bar{X}^n) = max(\sigma(\bar{X}^n) - \lambda, 0)$

Then we consider the Y **subproblem** in (6)

$$Y^{n+1} = \arg\min_Y \frac{1}{2}\|Y - Y^n\|_F^2 + I_{B_\infty}(Y) - t_2\lambda_1\langle\nabla(2X^{n+1} - X^n), Y\rangle, \quad (8)$$

After simplification, it becomes

$$Y^{n+1} = \arg\min_Y \frac{1}{2}\|Y - \bar{Y}^n\|_F^2 + I_{B_\infty}(Y), \quad (9)$$

where

$$\bar{Y}^n = Y^n + t_2\lambda_1\nabla(2X^{n+1} - X^n).$$

The solution of (9) can be obtained by the Euclidean projection of $\bar{Y}^n$ onto a ℓ_∞ unit ball, which could be evaluated by

$$Y^{n+1} = sgn(\bar{Y}^n) \cdot \min(|\bar{Y}^n|, 1), \quad (10)$$

where $sgn(x)$ is the sign function; it outputs 1 if $x > 0$, -1 if $x < 0$ and zero otherwise. All the operations in (10) are element-wise.

Now, the X, Y subproblems have been solved and we summarize the proposed FTVNNR in Algorithm 1. A key feature of the FTVNNR is its fast convergence performance. It can be proved that the ergodic convergence rate of FTVNNR is $\mathcal{O}(1/N)$ for N iteration [4].

Algorithm 1. FTVNNR

input: $\mathcal{A} = RF$, B, λ_1, λ_2
initialization: X_0, Y_0, t_1,t_2, $\lambda = t_1\lambda_2/(1 + t_1L)$
while not converged **do**
1) Compute: $\bar{X}^n = X^n - \frac{t_1}{1+t_1L}\mathcal{A}^T(\mathcal{A}X^n - B) - \frac{t_1\lambda_1}{1+t_1L}\nabla^T Y^n$ in (7)
2) Evaluate Matrix Shrinkage Operator: $X^{n+1} = S_\lambda(\bar{X}^n)$
3) Compute: $\bar{Y}^n = Y^n + t_2\lambda_1\nabla(2X^{n+1} - X^n)$ in (9)
4) Project $\bar{Y}^n$ onto ℓ^∞ unit ball: $Y^{n+1} = sgn(\bar{Y}^n) \cdot \min(|\bar{Y}^n|, 1)$ (element-wise)
end while

4 Experiments

4.1 Reconstruction Accuracy

We first evaluate our method on two noisy dynamic MR sequences. To simulate such noisy dynamic MR images, we use the in-vivo breath-hold cardiac perfusion ($128 \times 128 \times 40$) and cine data ($256 \times 256 \times 24$) from [16] and then add Gaussian white noise with standard derivation $\sigma = 0.05$ in the k-space data followed by the

equation (1). We apply the most practical Cartesian mask with 25% sampling ratio as the undersampling mask in our experiments. For quantitative evaluation, Peak Signal-to-Noise Ratio (PSNR) is adopted as the metric. All experiments are conducted using MATLAB 2013b on a desktop with 3.4GHz Intel core i7 4770 3.4GHz CPU and 16.0 GB RAM.

We compare our method with four state-of-the-art methods, the undersampled (k,t)-Space via Low-rank plus sparse prior (ktRPCA) [18], dictionary learning based method DLTG [2], the dynamic Total Variation (DTV) [5] and k-t SLR [12]. The source codes for these methods are downloaded from each author's website and we use their default parameter settings for all experiments. For the proposed method, we set $\lambda_1 = 0.001$ and $\lambda_2 = 3$ for both sequences.

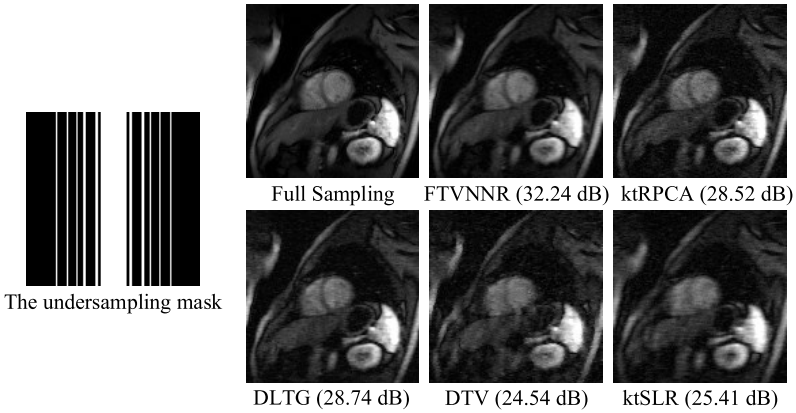

Fig. 1. Results of the 21st frame of the perfusion sequence at sampling ratio 1/4.

Fig. 1 shows the 21st reconstructed frame of the perfusion data. Clearly visible artifacts can be observed on the images by DTV and k-t SLR. Such results show that both methods are very sensitive to noise. Although it is reported that DTV gives very good performances [5], the method requires the reconstruction on the first frame to be very accurate, therefore it may not recover good results when there is no specific high sampling ratio for the first frame. Comparing the rest of the two approaches, DLTG reconstructs better results than ktRPCA. However, when looking at the time cost in Table. 1, one can see that DLTG requires nearly 2-3 hours for processing. Moreover, images obtained by both methods are still not very clear. Compared with the other four methods, the proposed FTVNNR can achieve the best reconstruction and cost the least amount of processing time.

Quantitative results of a whole sequence on two dynamic MR data are shown in Fig. 2. From the figure, one can clearly see that the proposed FTVNNR achieves the highest mean PSNR.

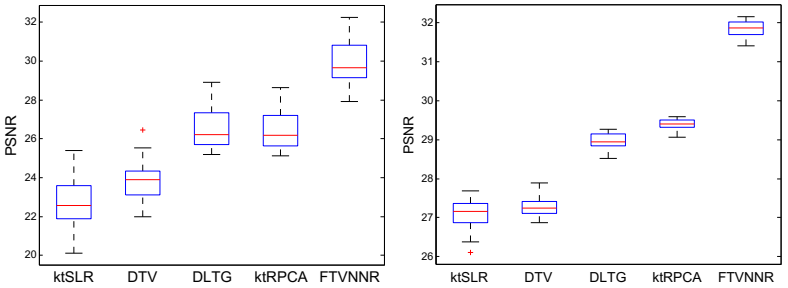

Fig. 2. Bxplot of PSNR results for (a) Perfusion data and (b) for Cine data. The proposed FTVNNR method outperforms all other methods being compared.

Table 1. The time cost of different methods

Time (Seconds)	Proposed	ktRPCA	DTV	k-t SLR	DLTG
Perfusion ($128 \times 128 \times 40$)	38	527	55	252	6614
Cine ($256 \times 256 \times 24$)	92	1282	121	609	11462

4.2 Multi-coil Parallel Imaging

To further evaluate performances, we use two multi-coil pMRI data from [16]; the number of coils is 12 and the coil sensitivities were known. The perfusion and cine data were acquired by Cartesian masks with 12.5% and 25% sampling ratio for all frames, respectively. We compare the proposed method with three state-of-the-art parallel MRI approaches including low-rank plus sparse reconstruction (L+S) [16], dynamic Total Variation (DTV) [5] and k-t SPARSE-SENSE [17].

The running time of all methods on the Perfusion and Cine data can be found in Table. 2. One can see that the proposed method has the fastest reconstruction speed compared to others, due to its fewer iterations and faster convergence.

Table 2. The time cost of different methods. "ktSS" is k-t SPARSE-SENSE

Time (Seconds)	Proposed	L+S	ktSS	DTV
Perfusion ($128 \times 128 \times 40$)	44.3	66.5	155.9	112.8
Cine ($256 \times 256 \times 24$)	56.5	78.9	115.5	291.9

Reconstruction results on the Cine data are shown in Fig. 3. All methods were able to reconstruct high quality images. However, when looking at details and temporal cross sections in Fig. 4, it can be observed that FTVNNR presents less noisy and lower residual aliasing artifacts on the cardiac surface. This is because the FTVNNR can utilize the local consistency in the spatial domain while the temporal FFT used in k-t SPARSE-SENSE and sparse prior in L+S can not exploit the spatial sparsity.

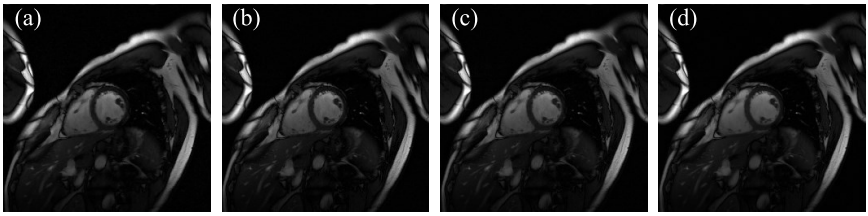

Fig. 3. Results of the 22nd frame of the Cine data. (a) DTV; (b) k-t SPARSE-SENSE; (c) L+S; (d) The proposed FTVNNR.

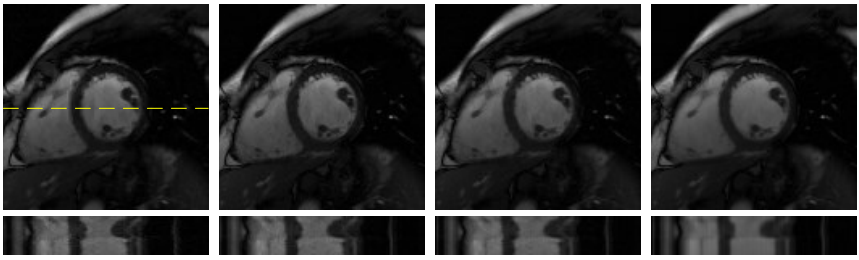

Fig. 4. Zoomed in areas of interest. The bottom are temporal cross sections by the yellow dashed line. From left to right are methods: (a) DTV; (b) k-t SPARSE-SENSE; (c) L+S; (d) The proposed FTVNNR.

5 Conclusion

We have proposed an efficient algorithm for dynamic MRI. The contributions of our work are as follows. First, the proposed FTVNNR achieves the best reconstruction performance when compared to four other state-of-the art methods. Second, it can obtain an $\mathcal{O}(1/N)$ convergence rate and experiments demonstrate that it is faster than other dMRI methods. These properties make the proposed method more powerful than conventional dMRI methods in terms of both accuracy and time efficiency. Moreover, the proposed method can be easily extended to parallel MRI. The parallel version of FTVNNR can also share good properties like fast convergence. Numerous experiments were conducted to show its better performance. In our future work, we will introduce existing online learning techniques [10,11] to further speed up the proposed FTVNNR and explore other applications in medical imaging.

References

1. Boyd, S., Vandenberghe, L.: Convex Optimization. Cambridge University Press, Cambridge (2004)
2. Caballero, J., Price, A.N., Rueckert, D., Hajnal, J.: Dictionary learning and time sparsity for dynamic MR data reconstruction. IEEE Transactions on Medical Imaging 33(4), 979–994 (2014)

3. Chambolle, A.: An algorithm for total variation minimization and applications. Journal of Mathematical Imaging and Vision 20(1-2), 89–97 (2004)
4. Chambolle, A., Pock, T.: On the ergodic convergence rates of a first-order primal-dual algorithm. Technical report, Optimization online preprint No. 4532 (2014)
5. Chen, C., Li, Y., Axel, L., Huang, J.: Real time dynamic MRI with dynamic total variation. In: Golland, P., Hata, N., Barillot, C., Hornegger, J., Howe, R. (eds.) MICCAI 2014, Part I. LNCS, vol. 8673, pp. 138–145. Springer, Heidelberg (2014)
6. Gamper, U., Boesiger, P., Kozerke, S.: Compressed sensing in dynamic MRI. Magnetic Resonance in Medicine 59(2), 365–373 (2008)
7. He, B., Yuan, X.: Convergence analysis of primal-dual algorithms for a saddle-point problem: From contraction perspective. SIAM Journal on Imaging Sciences 5(1), 119–149 (2012)
8. Huang, J., Zhang, S., Li, H., Metaxas, D.: Composite splitting algorithms for convex optimization. Computer Vision and Image Understanding 115(12), 1610–1622 (2011)
9. Huang, J., Zhang, S., Metaxas, D.: Efficient MR image reconstruction for compressed MR imaging. Medical Image Analysis 15(5), 670–679 (2011)
10. Li, Y., Chen, C., Huang, X., Huang, J.: Instrument tracking via online learning in retinal microsurgery. In: Golland, P., Hata, N., Barillot, C., Hornegger, J., Howe, R. (eds.) MICCAI 2014, Part I. LNCS, vol. 8673, pp. 464–471. Springer, Heidelberg (2014)
11. Li, Y., Chen, C., Liu, W., Huang, J.: Sub-selective quantization for large-scale image search. In: Proc. AAAI Conference on Artificial Intelligence (AAAI), pp. 2803–2809 (2014)
12. Lingala, S.G., Hu, Y., DiBella, E., Jacob, M.: Accelerated dynamic MRI exploiting sparsity and low-rank structure: k-t SLR. IEEE Transactions on Medical Imaging 30(5), 1042–1054 (2011)
13. Lustig, M., Donoho, D., Pauly, J.M.: Sparse MRI: The application of compressed sensing for rapid MR imaging. Magnetic Resonance in Medicine 58(6), 1182–1195 (2007)
14. Lustig, M., Santos, J.M., Donoho, D.L., Pauly, J.M.: k-t SPARSE: High frame rate dynamic MRI exploiting spatio-temporal sparsity. In: Proceedings of the Annual Meeting of ISMRM, p. 2420 (2006)
15. Ma, S., Goldfarb, D., Chen, L.: Fixed point and bregman iterative methods for matrix rank minimization. Mathematical Programming 128(1-2), 321–353 (2011)
16. Otazo, R., Cands, E., Sodickson, D.K.: Low-rank plus sparse matrix decomposition for accelerated dynamic MRI with separation of background and dynamic components. Magnetic Resonance in Medicine 73(3), 1125–1136 (2015)
17. Otazo, R., Kim, D., Axel, L., Sodickson, D.K.: Combination of compressed sensing and parallel imaging for highly accelerated first-pass cardiac perfusion MRI. Magnetic Resonance in Medicine 64(3), 767–776 (2010)
18. Trémoulhéac, B., Dikaios, N., Atkinson, D., Arridge, S.: Dynamic MR image reconstruction-separation from under-sampled (k,t)-space via low-rank plus sparse prior. IEEE Transactions on Medical Imaging 33(8), 1689–1701 (2014)